proceedings

MDPI

Proceeding Paper

Enhanced defect characterisation using pulsed phase thermography: The impact of sample geometry and signal-enhancement techniques †

Shayaan Saghir [1,*], Rachael C. Tighe [1] and Ye Chow Kuang [1]

[1] School of Engineering, University of Waikato, Hamilton 3216, New Zealand; ss957@students.waikato.ac.nz (S.S.); rachael.tighe@waikato.ac.nz (R.C.T.); yechow.kuang@waikato.ac.nz (Y.C.K.)

* Correspondence: ss957@students.waikato.ac.nz

† Presented at the 18th International Workshop on Advanced Infrared Technology and Applications (AITA), Kobe, Japan, 15–19 September 2025.

Abstract: In nondestructive evaluation (NDE), pulsed phase thermography (PPT) is a commonly used technique which relies on phase contrast to detect defects. This study presents a methodology to investigate how changes in signal processing and geometrical parameters affect phase contrast. Analytically simulated thermal signals are used to evaluate the phase contrast for varying sample thicknesses and defect sizes, relative to a fixed defect depth. To address the issue of spectral leakage, phase contrasts are recorded using both rectangular and Hamming windows before transformation into the frequency domain. A Gaussian process regression (GPR) modelling scheme is used to observe the relationship between phase contrast and geometrical parameters. The results suggest that both the choice of windowing function and geometrical factors can influence defect detection, offering insights to improve the reliability of PPT-based inspections.

Keywords: nondestructive evaluation (NDE); pulsed phase thermography (PPT); defect characterisation; noise reduction; phase enhancement

1. Introduction

The use of active infrared thermography (AIT) in the field of nondestructive evaluation (NDE) is becoming increasingly common due to its ability to rapidly detect subsurface defects. Among various AIT techniques, pulsed phase thermography (PPT) is a promising method to process raw thermograms by transforming the time domain data for each pixel into frequency domain, thereby enhancing the detection of deeper defects by reducing the effects of local surface emissivity variations and nonuniform heating [1]. One of the parameters of interest in PPT for defect characterisation is absolute phase contrast, which is evaluated across the frequency spectrum. This enables the detection of deeper defects at lower frequencies and shallower defects at higher ones. However, the efficacy of phase contrast is influenced by factors such as noise in raw thermal data and spectral leakage, especially when using a rectangular windowing function during Fourier transformation [2].

Previous studies have shown that geometrical parameters such as test sample thickness and defect size can cause discrepancies in detecting defects using pulsed thermography [3]. Investigating the effect of these parameters can help modify models for more

Academic Editor: Firstname Lastname

Published: date

Citation: To be added by editorial staff during production.

accurate defect detection. In the present work, it is examined how variations in defect size and sample thickness – relative to a fixed defect depth – influence the resulting phase contrast. To account for the influence of spectral leakage, two separate studies are conducted using different windowing functions. The following sections describe the methodology used to analyse the effect of these geometrical parameters on phase contrast, present the initial findings, and then conclude with some future objectives.

2. Effect of geometrical parameters on phase contrast

In this section, an overview is provided of the methodology adopted to observe the combined effect of two geometric parameters – sample thickness and defect size – on the phase contrast of defects. For this purpose, two parameters are defined: (a) the ratio of sample thickness to defect depth ($s = L/d$), and the ratio of defect size/diameter to defect depth ($r = D/d$). For analysis, ranges are defined for these two variables: s ranges from 1 (representing a defect-free slab) to 10, and r ranges from 1 to 20. The defect depth is assumed to be 1 mm.

To generate a sample space of different pairs of values for s and r, the Latin hypercube sampling (LHS) technique is used to evenly cover the specified ranges of these variables [4]. Figure 1 depicts the entire sample space created using the LHS strategy, where a wide spread of s and r over the defined ranges can be observed. Using this sample space, the absolute phase contrast corresponding to each pair of values is evaluated to create the dataset for input into the Gaussian process regression (GPR) model.

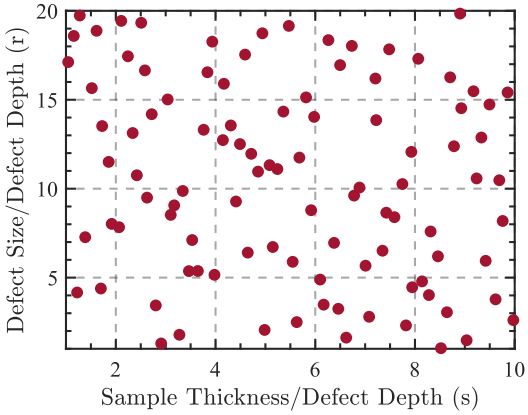

Figure 1. Scatter plot of the sample space generated using the Latin hypercube sampling (LHS) method.

2.1. Estimation of phase contrast

The estimation of phase contrast for each set of variables is based on evaluating the temperature signals for regions above both the sound (reference) area and the defect. For this, analytical solutions are used for both the reference region and a defect of diameter D. If, at $t = 0$, an instantaneous heat pulse with energy density Q_0 is provided on the surface of a homogenous plate of thickness L, containing a circular defect at a depth d, then the surface temperature changes on the front surface for the regions above both the reference and the defect can be approximated as [5]:

$$\Delta T_r(0,t) = \frac{Q_0}{e_m\sqrt{\pi t}}\left[1 + \sum_{n=1}^{\infty} R^n e^{-(nL)^2/\alpha t}\right] \quad (1)$$

$$\Delta T_d(0,t) = \frac{Q_0}{e_m\sqrt{\pi t}}\left[1 + \sum_{n=1}^{\infty} R^n e^{-(nd)^2/\alpha t}.\left(1 - e^{-(D)^2/16\alpha t}\right)\right] \quad (2)$$

In the above equations, ΔT_r and ΔT_d are surface temperature changes (at $x = 0$), α $(= k/\rho C)$ is the thermal diffusivity, and $e_m (= \sqrt{k\rho C})$ is the thermal effusivity with k, ρ and C being the thermal conductivity, density and specific of the material, respectively. The term R is the thermal wave reflection coefficient, which is set at 1 (air interface) for simplicity. To make the data more realistic, random noise with standard deviation of 25 mK is added, considering the NETD of IR cameras.

For the estimation of absolute phase contrast, a modified pulsed phase thermography algorithm, as proposed by Netzelmann and Müller [6], is adopted to reduce computation time and minimise noise at higher analysis frequencies. The implementation is based on the fast Fourier transform (FFT) algorithm and uses only the first component (after the DC component) at each transformation step. The algorithm is as follows:

$$F_k^{modPPT} = \sum_{n=0}^{Round(N/k)-1} T_n e^{-i2\pi n/Round(N/k)} \quad k > 0 \tag{3}$$

After applying the algorithm, the transformed signal F_k is obtained. Using the imaginary part of equation (3), the phase delay of the transform is then calculated. Subsequently, the absolute phase contrast $\Delta\emptyset = \emptyset_d - \emptyset_r$ is computed, where $\emptyset_d$ and $\emptyset_r$ are the phase contrasts for the temperature signals obtained from equations (1) and (2), respectively.

2.2. Gaussian process regression (GPR)

To analyse the effect of changes in sample thickness and defect diameter along with the influence of windowing function on phase contrast, analytically simulated temperature signals were generated for each pair of values in the LHS-based sample space under two conditions. In the first case, a rectangular window was used, whereas in the second, a Hamming window was used prior to transforming the data into the frequency domain. The phase contrast is then estimated using the PPT algorithm, as described by equation (3). For both cases, the absolute maximum phase contrast was considered for each (s, r) pair.

After preparing the datasets, a Gaussian process regression (GPR) model is fitted using a squared exponential kernel function [7]. The developed regression model for each case was then used to predict phase contrast values over a test space of s and r to study their relationship with phase contrast.

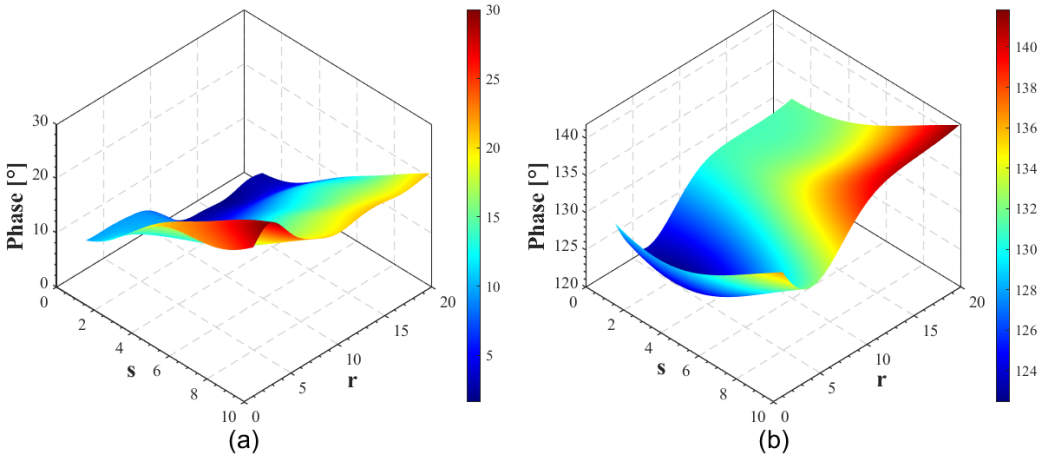

Figure 2. 3D surface plots of phase contrasts as a function of sample thickness to defect depth (s) and defect size to defect depth (r) ratios using Gaussian process regression (GPR) for the case of (**a**) rectangular window; (**b**) Hamming window.

Figure 2a shows the surface plot of phase contrast as a function of s and r when a rectangular window is used. It can be observed that, for a given value of r, the phase contrast improves with increasing s. In other words, for a defect located at a certain depth in a thicker sample, the phase value becomes greater compared to the same defect present in a thinner sample. On the other hand, Figure 2b shows a different trend when a Hamming window is used. In this case, the phase contrast decreases nonlinearly with decreasing r until a certain point and then increases again as r approaches its minimum value. Another aspect is that for different defect sizes, the same phase contrast can be obtained, which can lead to misinterpretation in defect quantification.

3. Conclusions

For defect detection using PPT, phase contrast is affected by changes in both geometrical and signal processing parameters. This study has analysed how simultaneous variations in sample thickness and defect diameter – relative to a fixed defect depth and windowing function – impact the resulting phase contrast, thereby affecting the interpretation and reliability of defect detection. These results highlight the importance of adapting signal processing methods to consider the geometrical characteristics of the inspected sample. In future work, further investigation is planned into the behaviour of phase contrast under different processing parameters, including validation using experimentally collected data.

Author Contributions: Conceptualisation, R.C.T. and S.S.; methodology, S.S., R.C.T. and Y.C.K.; software, S.S. and R.C.T.; validation, R.C.T. and Y.C.K.; formal analysis, S.S. and R.C.T.; investigation, S.S..; writing—original draft preparation, S.S.; writing—review and editing, R.C.T. and Y.C.K.; visualization, S.S.; supervision, R.C.T. and Y.C.K.; project administration, R.C.T.; funding acquisition, R.C.T. All authors have read and agreed to the published version of the manuscript.

Funding: This research is supported by Royal Society Te Apārangi, New Zealand under Marsden Fund Council with grant no. UOW2103.

Institutional Review Board Statement: Not applicable.

Informed Consent Statement: Not applicable.

Data Availability Statement: Data can be obtained from authors on request.

Conflicts of Interest: The authors declare no conflicts of interest.

References

1. Ibarra-Castanedo, C.; Maldague, X. Pulsed phase thermography reviewed. *Quant. Infrared Thermogr. J.* **2004**, *1*, 47–70.
2. Olafsson, G.; Tighe, R. C.; Dulieu-Barton, J. M. Improving the probing depth of thermographic inspections of polymer composite materials. *Meas. Sci. and Technol.* **2018**, *30*, 025601.
3. Wei, Y., Zhang, S., Luo, Y., Ding, L., & Zhang, D. (2021). Accurate depth determination of defects in composite materials using pulsed thermography. *Composite Structures*. **2021**, *267*, 113846.
4. Viana, F.A. A tutorial on Latin hypercube design of experiments. *Qual. Reliab. Eng. Int.* **2016**, *32*, 1975–1985.
5. Almond, D.P.; Pickering, S.G. An analytical study of the pulsed thermography defect detection limit. *J. Appl. Phys.* **2012**, *111*, 093510.
6. Netzelmann, U.; Müller, D. Modified pulse-phase thermography algorithms for improved contrast-to-noise ratio from pulse-excited thermographic sequences. *NDT E Int.* **2020**, *116*, 102325.
7. Williams, C.K.; Rasmussen, C.E. *Gaussian Processes for Machine Learning*; MIT Press: Cambridge, MA, USA, 2006; Volume 2.